An Introduction to the 1997 ESA MASTER Model

H. Klinkrad*, J. Bendisch**, H. Sdunnus***, P. Wegener**, and R. Westerkamp**

* ESA/ESOC, Darmstadt, Germany
** TUBS/IFR, Braunschweig, Germany
*** HTS AG, Wallisellen, Switzerland

Abstract

In 1995 ESA distributed a β-version of their meteoroid and space debris terrestrial environment reference model (MASTER) to a limited number of reviewers. Resulting improvements and new developments have been merged into a first MASTER release version which will be introduced in this paper. The MASTER model is based on quasi-deterministic principles, using comprehensive orbit propagation theories and volume discretisation techniques to derive spatial densities and velocity distributions in a 3D control volume ranging from LEO to GEO altitudes. The particulate environment is derived for objects larger than 0.1 mm. Space debris are generated for 132 historic fragmentation events, and they are propagated to a reference epoch of 31-Mar-1996. At this time the debris are merged with the non-fragment catalog population. Meteoroids are retained for the core and asteroidal populations of the Divine/Staubach model at 1 AU. Collisional flux from debris and meteoroids can be analysed with high information content of results for arbitrary, user defined target orbits in the MASTER Analyst version. For moderately eccentric target orbits flux results of the same accuracy but with reduced information content can be computed with a CPU time efficient MASTER Engineering version. The entire MASTER model, including executable code, data files, documentation, and auxiliary software, is distributed for a wide range of computer platforms on a single 680 MByte CD ROM. The MASTER CD ROMs will be available to interested users as of May 1997.

1. Introduction

Today, in March 1997, the Space Surveillance Network (SSN) of the US Space Command (USSPACECOM) is routinely tracking, correlating, and cataloging some 8,300 objects between low earth orbit (LEO) and geostationary (GEO) altitudes. Due to limitations in the sensitivities of the radar and electro-optical SSN sensors, the detection threshold ranges from 10 cm diameters in LEO to 1 m diameters in GEO and the GEO transfer orbits (GTO). Experimental observation campaigns with advanced radar and optical sensors indicate that at the lower end of the SSN detection threshold the catalog population may be incomplete by up to a factor 2 (also know as "Henize Factor"). In particular, a large population of cm-size objects was observed at altitudes between 700 and 1000 km, in high inclination orbits. Reflection properties and radar polarization signatures indicate that these may be Na-K droplets which could have escaped from the more than 30 nuclear reactors which have been raised to these deposit orbits at the end of Russian RORSAT missions.

The current catalog population of 8,300 is the remainder of almost 24,800 space objects which have been tracked and correlated to date. The other 16,500 objects have decayed under the influence of airdrag, with increased removal rates from LEO at times of high solar activity. The on-orbit objects, which are the result of about 3,800 launches so far, can be classified as spent upper stages (16%), defunct satellites (20%), and only 6% operational payloads. With 53%, however, the majority of the catalog objects, and nearly all uncatalogued subdecimeter objects are originating from 136 on-orbit fragmentations since 1961. With the exception of 2 or 3 collisions, all these were accidential or deliberate explosions of satellites or rocket upper stages. One of the most recent events, the explosion on 03-Jun-1996 of a Hydrazine Auxiliary Propulsion System (HAPS) of a Pegasus rocket (1994-029B) caused 700 trackable fragments from an original mass of 97 kg. Also recently, on 24-Jul-1996, the first collision between two catalog objects was recorded when the gravity gradient boom of the French Cerise satellite (1995-033B) was severed by a fragment (86-019RF) of an Ariane-1 upper stage explosion. While such conjunction events can be predicted with a certain probability by means of deterministic methods, the collision risk from the far more abundant non-trackable and also non-shieldable objects of diameters 1 cm $\leq d \leq$ 10 cm (expected to be 8 to 20 times the catalog population) must be assessed by statistical methods. The ESA MASTER model uses such concepts to predict the debris collision flux for a given earth orbit and for a given mass or size threshold of the impactor.

The MASTER model has been developed under ESA contracts with TU Braunschweig and Battelle Germany, and with own ESA contributions in the past few years (Ref.7). The model covers space debris and meteoroids of diameters $d \geq 0.1$ mm, and it is applicable to any earth orbit between 185 km and the geostationary ring. The modeling approach, the structure of the MASTER model, and the concept of its CD ROM implementation will be explained in the following.

Proceedings of the Second European Conference on Space Debris, ESOC, Darmstadt, Germany, 17-19 March 1997, (ESA SP-393, May 1997)

2. The MASTER Debris Model

2.1 Concept of the Debris Model

MASTER, ESA's meteoroid and space debris terrestrial environment reference model, is a collision risk assessment tool for debris and meteoroids which is applicable to any terrestrial target orbit between 185 km and super-GEO altitudes. The MASTER model concentrates on objects larger than 0.1 mm. For man-made debris a corresponding population of about 10^{+11} particulates is generated by modeling 127 fragmentation events (with 66 high intensity explosions, and 2 collisions). These 127 modeled events account for 132 registered events up to the MASTER reference epoch of 31-Mar-1996. The difference is due to multiple explosions of objects from the same source. The mass distribution for each fragmentation is determined to fit the observable, cataloged number of objects from the event (according to data from Ref.1, augmented with NASA information after July 1995), with the lower end of the mass spectrum of MASTER (at $d \approx 0.1$ mm) adjusted to match the impact statistics on space exposed hardware (LDEF, EURECA, HST). Based on spatial object densities, the equivalent MASTER population in LEO consist of about 150,000 objects larger than 1 cm.

In order to reduce the total number of about 10^{+11} generated fragments of $d > 0.1$ mm, objects of common properties are grouped, and one representative fragment receives a weight factor corresponding to the group extent. This factor ranges from 1 in case of trackable sizes to 10^{+3} at the 0.1 mm model threshold. The representative population is thus reduced to 232,600 objects, which are propagated to a common reference epoch (31-Mar-1996 for the present release) by means of a comprehensive orbit perturbation theory. The orbit prediction considers the zonals of the geopotential J_2, J_3, J_4, $J_{2,2}$, third body attraction due to sun and moon, airdrag as a function of observed solar activity, and solar radiation pressure effects for an oblate earth shadow. The numerical integration of the corresponding singly averaged equations of motion takes considerably less than 1 sec of CPU time per object and year. The evolution history of individual debris clouds can be followed to generate a time profile of their contribution to the overall population.

The ensemble of 232,600 propagated, representative (weighted) objects at reference epoch 31-Mar-1996 is subjected to a discretisation process, where each individual orbit is checked for passes through cells of a spherical control volume which is deployed around the earth in altitude (ΔH), latitude ($\Delta\delta$), and right ascension ($\Delta\alpha$) of an earth centered, equatorial system of date. The current MASTER implementation uses three distinct regimes for low earth orbits (LEO), medium earth orbit (MEO), and the geostationary ring (GEO), with the following segmentations and pass statistics:

- LEO environment: altitudes from 185 km to 2,285 km, with $\Delta H = 10$ km, $\Delta\delta = 2°$, and $\Delta\alpha = 10°$; number of modeled objects passing through LEO: 137,000
- MEO environment: altitudes from 2,285 to 34,785 km, with $\Delta H = 500$ km, $\Delta\delta = 2°$, and $\Delta\alpha = 360°$ (right ascension averaging); number of modeled objects passing through MEO: 185,000
- GEO environment: altitudes from 34,785 to 36,785 km, with $\Delta H = 10$ km, $\Delta\delta = 1°$ (latitude band: $\delta \in [-15°, +15°]$), and $\Delta\alpha = 10°$; number of modeled objects passing through GEO: 88,000

For each pass by a debris orbit through a cell of the spherical control volume, the resident probabilities (based on cell dwell time in relation to the orbit period), spatial density contributions, and transient velocities (both magnitude and direction) are determined in horizontal coordinates of an inertial, earth-centred, equatorial system (Ref.5). The cell passage events (CPEs) are then translated to the central cell position, and they are stored cell-wise, with details on the source (catalog number), mass (size), and orbit elements of the objects retained. In order to compute collision fluxes for a given target trajectory, based on discretised 3D debris distributions, intersections of the target orbit with all control volume cells during one revolution are determined. For each cell passage, all previously stored information on debris passes is retrieved, and for each particulate the incremental collision flux contribution is determined from the relative velocity, the spatial density, and the resident probability. Full details on the flux direction (in terms of azimuth and elevation in a target centered orbit system), collision velocity, and impactor properties (mass, origin, and orbit) are available for a subsequent analysis. Optionally, the cell passage event (CPE) information can be evenly distributed along small circles of latitude (averaging over right ascension). This is the default used in the MEO region to guarantee a sufficient number of passage events per volume cell. In total, there are 1,114,740 volume cells which on the average have 69 orbit passes, yielding a total of 70,026,040 cell passage events for the whole MASTER debris model.

The debris flux determination procedure described so far is called the "Analyst Mode". In this mode results are obtained which reflect the full information scope offered by MASTER, and which are valid for any earth orbit including highly eccentric ones (e.g. GTOs). As a derivative of the Analyst Mode, an "Engineering Mode" has been devised which is limited to near circular and moderately eccentric target orbits, which uses CPEs averaged over right ascension, but which is orders of magnitude faster in computer implementations than the Analyst Mode. The Engineering Mode is based on table look-up and interpolation techniques, where each grid point of the table is generated by a run in the Analyst mode for circular orbits of given inclination and mean altitude, and for a given size threshold of the impactors. Moreover, along the target orbit, at positions optimised with respect to the spatial density distribution with latitude, impact directions and velocities are retained to allow for a position dependent flux analysis. Moderate eccentricities are accounted for by interpolation of flux results for velocities $V_{e=0}$ and $V_{e=0} \pm 0.5$ km/s at given locations $u = \omega + f$ along the orbit. Depending on the target orbit, the execution time of the Engineering Model can be up to 500 times shorter than for the Analyst Model.

2.2 Results of the Debris Model

The high resolution Analyst version of the MASTER model can be applied to any earth orbiting spacecraft between 185 km and GEO altitudes. Five examples shall demonstrate the high information content of corresponding results for the International Space Station ISS,

for the ERS-1 earth observation satellite, for an Ariane-5 upper stage on a GTO orbit, for Meteosat-5 in a GEO orbit, and for a satellite from the Iridium constellation. All subsequent debris results have been generated for non-shieldable objects of $d1$ cm, for a reference epoch of 01-Jan-1997, and for cell passage events averaged with respect to right ascension.

Fig.1 shows the collision flux for the International Space Station (ISS) on its orbit of $H = 450$ km, $e = 0.001$, and $i = 51.5°$, as a function of the orbit position $u = \omega + f$ and of the impact azimuth A (where $A = 0°$ denotes the flight direction). A sinusoidal variation of left hand and right hand flux contributions from descending and ascending debris orbits is noticeable, with peak fluxes at the extreme declinations. Due to the lack of retrograde debris orbits of $i > 110°$ a gap within $A = \pm 10°$ is remaining in the impact azimuth distribution. At node crossings a wider spread of $F(u,A)$ in azimuth is due to objects from GTOs. The ISS azimuth distribution translates into a corresponding impact velocity pattern as shown in Fig.2. The dark structures relate to the 65° and 98° debris inclinations. For the ERS-1 satellite, on its sun-synchronous orbit at $H = 780$ km and $i = 98.5°$, Fig.3 shows debris flux versus argument of true latitude u and collision azimuth angle A. Since most debris orbits are prograde, the near-polar ERS-1 orbit has almost all impacts from the left hand side on ascending arcs and from the right hand side on descending arcs. Maximum flux occurs during passes of declinations which correspond to densely populated inclination bands (see also Fig.14). Signatures of these distinct populations are visible as closed contours also in the resulting collision velocity distribution along the orbit (Fig.4), where V has a most probable value of 15 km/s due to the most frequent near head-on collisions with orbits of 82° and 74° inclination (see Fig.5). In Fig.11 and 12 debris flux results are summarised for a single satellite (out of 77) of the future Iridium constellation, with $H = 760$ km, $e = 0.001$, and $i = 88°$. The collision azimuth and impact velocity distribution along the orbit shows similar features as for ERS-1, with more pronounced ring structures visible in both charts as a finger print of the most densely populated inclination bands.

As an example of a GEO case, Fig.6 shows the azimuth and elevation distribution of debris flux for the Meteosat-5 orbit at $H = 35{,}786$ km, for $i \approx 0°$. Collision azimuths are mainly grouped around $A = \pm 90°$ due to low velocity rendez-vous collisions with co-orbiting objects (at $V \leq 0.8$ km/s), and around $\pm 40°$ due to collisions with debris from from Molniya-type highly eccentric orbits of 65° inclination at velocities of 3 km/s. One of the most complex scenarios is displayed in Fig.7 to 10 for an Ariane-5 GEO transfer orbit of $H_{pe} = 585$ km, $e = 0.718$, $i = 7°$, and $\omega = 178°$. In Fig.7 the impact flux is shown as a function of collision azimuth A and orbit position angle u. Due to missing debris populations in complementary inclinations bands most of the collisions are under azimuth angles outside $A = \pm 15°$. The majority of the flux is collected while passing the densely populated altitude region between 800 km and 1000 km altitude ($u \approx 25°$) at velocities around 10 km/s ($A \approx 20°$). The flux sub-maxima at $A \approx 15°$ can be attributed to low inclination orbits which are swept up by the high GTO perigee velocity. In the GEO vicinity, the GTO target object is either caught up by GEO objects from $A = 180° - i_{gto} \pm 15°$, or it is hit in rendez-vous collisions (with $A = \pm 90°$) by co-orbiting GTO fragments. Fig.8 shows the collision elevation angle distribution along the GTO. On the ascending arc debris are encountered from the top ($h > 0°$) under increasing angles, until the GEO region is entered. Due to low encounter velocities in this regime, impacts are occurring under all elevation angles. On the descending arcs the impact elevations change their sign. In Fig.9 the encounter velocities along the GTO trajectory are shown, where areas of high flux can be correlated with impactor inclination bands depicted in Fig.10. Hence, debris orbits at $i = 65°$ and $i = 98°$ yield maximum impact velocities around 11 km/s and 14 km/s, respectively.

In the MASTER Engineering model the cell-wise debris flux information is averaged with respect to right ascension, and the particulate flux for a near circular target orbit is interpolated from tabled information with grid points specified by mean orbit altitude, inclination, orbit location $u = \omega + f$, and impactor size or mass threshold. Fig.13 shows the total flux for debris of sizes $d > 1$ cm as a function of altitude and inclination of a target orbit. Peak fluxes can be noted for sun-synchronous inclinations at $H = 900$ km, and 1500 km as a consequence of the orbital distribution of the historic fragmentation events. This orbital distribution of fragmentations also shapes the spatial densities in LEO which are displayed in Fig.14. Densely populated inclination bands determine the maxima along latitude profiles of constant altitude, while common fragmentation altitudes create density peaks on altitude profiles along small circles of latitude.

3. The MASTER Meteoroid Model

3.1 Concept of the Meteoroid Model

The MASTER meteoroid model is based on Divine's theory (Ref.2) of five distinct populations with specific signatures in terms of mass spectrum, and of eccentricity, inclination, and perihelion distance in an ecliptic reference system. The Divine model consists of a core population, with heliocentric orbits of small i_{core} and e_{core}, and mean masses of about $\overline{m}_{core} \approx 10^{-5}$ g, an eccentric population with large e_{ecc}, small i_{ecc}, and $\overline{m}_{ecc} \approx 10^{-12}$, an inclined population with large i_{inc} and small i_{ecc}, and $\overline{m}_{ecc} \approx 10^{-8}$, a halo population with small e_{halo}, random i_{halo}, and $\overline{m}_{halo} \approx 10^{-7}$, and an asteroidal population with small e_{ast} and i_{ast}, highest concentrations near the asteroid belt, and mean masses of $\overline{m}_{ast} \approx 10^{-3}$. In the past years the Divine model has been extended and modified mainly for small size particulates by Staubach (Ref.8), using new data from the Ulysses and Galileo impact detectors. The former eccentric, inclined and halo populations are denoted as A, B, and C populations in Staubach's extended model. The probability distributions in ecliptic inclination and heliocentric eccentricity of the populations used in the Staubach model are shown in Fig.17 and 18. For the given 0.1 mm size threshold of the MASTER model mainly the core and asteroidal meteoroids provide flux contributions. Both of these populations have prograde inclinations, predominantly below 20°, and their orbit eccentricities are typically below 0.7. The peak density of the asteroidal meteoroids is near 2.5 AU, whereas the core population shows a nearly uniform distribution with heliocentric distance.

For the MASTER model, the relevant meteoroid orbits are generated according to known distribution functions for mass, perihelion, eccentricity, and inclination (see

Fig.17 and 18), with uniformly distributed node and perihelion positions. To derive spatial density contributions and absolute velocities, an earth-centred spherical control volume is deployed with segmentations in right ascension and declination defined in an ecliptic system with $\alpha_{ecl} = 0°$ towards the sun direction (corresponding to 12 h mean local solar time), and δ_{ecl} measured with respect to the ecliptic plane. This reference system has the advantage that the computed meteoroid cell passage events have a uniform distribution during a one year cycle, and symmetries can be used to reduce the number of stored cells to one quarter of the original volume. The reference control volume for altitudes from 185 km to 38,185 km is discretised into 7 concentric shells of $\Delta H = 400$ km to 10,000 km, 4 zonals partitions of $\Delta\delta_{ecl} = 22.5°$ for $\delta_{ecl} \in [0, 90°]$, and 8 tesseral partitions of $\Delta\alpha_{ecl} = 22.5°$ for $\alpha_{ecl} \in [0, 180°]$. This coarser grid as compared with the space debris control volume is justified by the reduced sensitivity of results with respect to position changes in H, α_{ecl}, and δ_{ecl}. For each spherical sector of the control volume there are exactly 16,380 CPEs describing the flux in 180 azimuth and 91 elevation classes. This corresponds to more than $14 \times 10^{+6}$ meteoroid CPEs in total.

For meteoroid flux computations a terrestrial target orbit is firstly translated into the rotating ecliptic, sun-oriented coordinate system. In this system cell passage events are determined for the target object, and flux contributions are cumulated along the orbit in a similar way as for the debris model. Results are then translated into the common earth-centred, inertial, equatorial coordinate system. Earth shielding and gravitational focussing effects are taken into account as defined by Divine and Staubach (Ref.8). As was the case for the MASTER debris model, also the meteoroid model is available in a high-resolution Analyst mode, with no constraints on the target orbit shape, and in a CPU optimised Engineering mode which is limited to near circular and moderately eccentric orbits.

3.2 Results of the Meteoroid Model

In Fig.15 the spatial resolution of the new MASTER meteoroid model is illustrated. The flux of meteoroids of $d > 0.1$ mm is shown in a right ascension and declination grid for a target which is 20,000 km behind the earth on its orbit around the sun (α_{ecl} measured from the sun direction, inside the ecliptic plane, and δ_{ecl} measured perpendicular to the ecliptic). The earth is located at $\alpha_{ecl} = -90°$, covering a cone of 36° width. The corresponding shielding effect is clearly noted in the flux distribution which has maxima under $\alpha_{ecl} = 20°$ and 160°, with δ_{ecl} mainly within $\pm 40°$. These patters are a consequence of the orbit distributions of the core and asteroidal meteoroid populations.

Fig.16 shows the distribution of relative velocities of the MASTER meteoroid model in an earth fixed reference system as a function of the geocentric radial distance. The velocity distribution proposed by Kessler is superimposed as a solid curve. Kessler's distribution best fits the MASTER results for an altitude near 400 km. With increasing radial distance, the core and asteriodal meteoroids used by MASTER create a wider spread of the velocity probability function, with a lower peak density near 11 km/s, and larger contributions from the low velocity sprectrum between 3 and 10 km/s.

4. Verification of Model Assumptions

Except for 2 or 3 collisions, the 132 fragmentation events accounted for by the MASTER model are due to explosions of spent upper stages or of satellites. In order to verify and improve existing mathematical methods to model such events, the German Battelle Institute conducted three ground based explosion tests on 1:5 downscaled, simplified mock-ups of an Ariane H-10 upper stage. The cylindrical tanks were filled with a stoichiometric H_2/O_2 mixture of temperatures and pressures determined according to similarity laws. The explosive inventory for the three test cases ranged from a TNT equivalent mass on 1.3 kg to 2.1 kg. Using diagnostic equipment like flash X-ray photography, and high speed cameras, fragment velocities of up to 600 m/s could be measured (with flame expansion velocities up to 1000 m/s). Soft catcher devices around the test articles allowed to retrieve fragments which were binned according to masses. The mass spectrum was upscaled to the H-10 original dimensions, and it was then used to adjust the lower end of the mass distribution functions used in MASTER (Ref.3).

The Analyst Model of MASTER can also be used in an 'observatory mode', where for a given radar location, defined system parameters, and a certain observation volume the detection statistics are predicted for a longitude-averaged debris distribution. The β-version of MASTER was tested in this mode against measurement data from 345 hours of Haystack observations (X-band) and from 24 hours of FGAN observations (L-band), both in zenith staring mode with a range gate defining a volume around 800 km altitude. Using detection thresholds of $d > 5$ mm for Haystack and $d > 3.3$ cm for FGAN, the MASTER over-predicted the Haystack detections by a factor of 5, and underestimated FGAN detections by the same magnitude (Ref.6). The discrepancies in these results can probably be attributed to deficiencies in translating radar system performance parameters to detection thresholds. For the current release of MASTER, the related algorithms will be improved.

At its lower size threshold of 0.1 mm diameters the MASTER model can be verified against particulate impact statistics derived from space returned hardware (Ref.6). The EURECA spacecraft and the retrieved solar array of the Hubble Space Telescope (HST) are particularly well suited for such a comparison, because their data are recent (Jul.92 to Jun.93 for EURECA, and Apr.90 to Dec.93 for HST), and sufficiently close to the MASTER reference epoch of Mar.97 . EURECA, operating for almost 1 year at an orbit altitude between 340 km and 520 km, and at an inclination of 28.5°, showed 970 impacts of diameters larger than 0.1 mm, spread over a total exposed surface of 140 m². The largest impact feature measured 6.4 mm across. The observed EURECA impact rate for $d > 0.1$ mm agrees well with the MASTER prediction at its lower model threshold. This holds also true for a comparison with impact statistics of the HST solar array, which was retrieved from an altitude near 610 km and an inclination of 28.5° after 3.62 years of space exposure. Since the impact statistics for 0.1 mm objects are dominated by meteoroids (with less than 10% space debris), the EURECA and HST data mainly serve as a validation of the meteoroid flux model of Divine and Staubach (Ref.8) which is used within MASTER.

5. MASTER Distribution on CD ROM

A β-release of the MASTER model was distributed in mid 1995 to a number of debris researchers worldwide. A release version of MASTER, with extended capabilities and worked-in suggestions from β-users, will become available in May 1997. The MASTER model is contained on a single 680 MByte, ISO 9660 partitioned CD ROM, including all user documentation, data files, executables, and auxiliary software for a wide range of computer platforms and operating systems. Apple users, with System 7 operating system, receive an additional Apple formatted diskette which contains executables (resource forks) which are incompatible with the ISO 9660 CD partition. Most of the CD ROM is occupied by 500 MBytes of cell passage event data (CPEs). Custom, multi-step data compression techniques with compression ratios of about 1:7 had to be developed to condense to original volume of about 85,000,000 CPE data records to the available CD ROM allocation.

The executable codes and data files of the MASTER CD ROM are compatible with most of the common computer platforms and operating systems, including RS-6000 (AIX), PCs (386 or later, and Pentium with DOS or Windows), HP-9000 (HP Unix), SUN SPARC (SUN OS or Solaris), VAX (VMS), and Apple (System 7). The CD ROM also contains the GNUplot plotting software, which can be directly used to visualised MASTER results via pre-defined scripts, and the GhostView PostScript software, which can be used to view and print-off the included PostScript formatted user manuals. To get an idea of possible application scenarios of MASTER, five complete test cases (with input and output files) are provided for an ERS-1 sun-synchronous target orbit, for an Ariane-5 GTO orbit, for a Meteosat-5 GEO orbit, and for two post processor options of MASTER: a computation of detection statistics of the FGAN radar during LEO observation, and a determination of debris flux on an inertially fixed unit sphere at 800 km altitude and 82° declination.

6. Summary and Conclusions

ESA's meteoroid and space debris terrestrial environment reference model (MASTER) is based on quasi-deterministic methods to generate and propagate fragments from more that 130 on-orbit explosions and collisions, which are used to derive spatial object densities and transient velocities in a discretised spherical control volume extending from LEO to GEO altitudes. Collision fluxes on target orbits can then be determined by interrogation of the information of intersected segments of the discretised volume. In a similar way spatial densities and resulting collision fluxes can be determined for meteoroids. The current MASTER model only takes into account man-made and natural objects larger than 0.1 mm. In future releases the model will be extended to smaller sizes ranges, taking into account so far unmodeled populations due to cm-size objects observed near 900 km altitude, due to paintflakes and surface degradation, and due to slags from solid rocket motor firings.

The MASTER model is distributed on a single, 680 MByte, ISO formatted CD ROM which is compatible with most common computer platforms and operating systems, and which contains all necessary data files, executable codes, and documentation to perform collision flux analysis for arbitrary, user defined target orbits. The software comprises an Analyst Version with no constraints on target orbits and with a high information content in the output results, and a more CPU time efficient Engineering Version, limited to moderately eccentric orbits, which generates flux results of the same accuracy, but with lower resolution.

The MASTER model CD ROM (1997 release) will be distributed by ESA/ESOC as of May 1997. Requests can be submitted to the first author.

Acknowledgement

The contributions to the MASTER meteoroid model by P. Staubach (formerly MPI Heidelberg), and F. Wilms (TU Braunschweig) are gratefully acknowledged.

References

1. I.W. Grissom, G.A. Myers
History of On-Orbit Satellite Fragmentations (9th Edition), TBE Technical
Report **CS95-LS-024** , 1995

2. N. Divine, E. Gruen, P. Staubach
Modeling the Meteoroid Distributions in Interplanetary Space and Near Earth
Proceedings **ESA SD-01** , 1st European Conf. on Space Debris, pp. 245-250, Darmstadt, Germany, 5-7 April, 1993

3. W. Fucke
Fragmentation Experiments for the Evaluation of the Small Size Debris Population
Proceedings **ESA SD-01** , 1st European Conf. on Space Debris, pp. 275-280, Darmstadt, Germany, 5-7 April, 1993

4. S. Hauptmann
A Comparison of ESA and NASA Space Debris Models
ESA Symposium on Environment Modeling for Space-Based Applications, ESA/ESTEC, Noordwijk, The Netherlands, Sep. 18-20, 1996

5. H. Klinkrad
Collision Risk Analysis for Low Earth Orbits
Advances in Space Research , Vol.13, No.8, pp.177-186, 1993

6. H. Klinkrad, W. Flury, H. Sdunnus, D. Rex
Use of Debris Measurement Data for Verification and Improvement of the ESA MASTER Model
International Workshop on Space Debris, Moscow, Russia, Oct. 9-11, 1995

7. H. Sdunnus,
The ESA Meteoroid and Space Debris Terrestrial Environment Reference Model (MASTER)
Final Report, ESA contract no. **10453/93/D/CS** , Darmstadt, Germany, 1995

8. P. Staubach;
Upgrade of the DISCOS Meteoroid Model, Final Report, ESA contract no.
10463/93/D/CS , Darmstadt, Germany, 1996

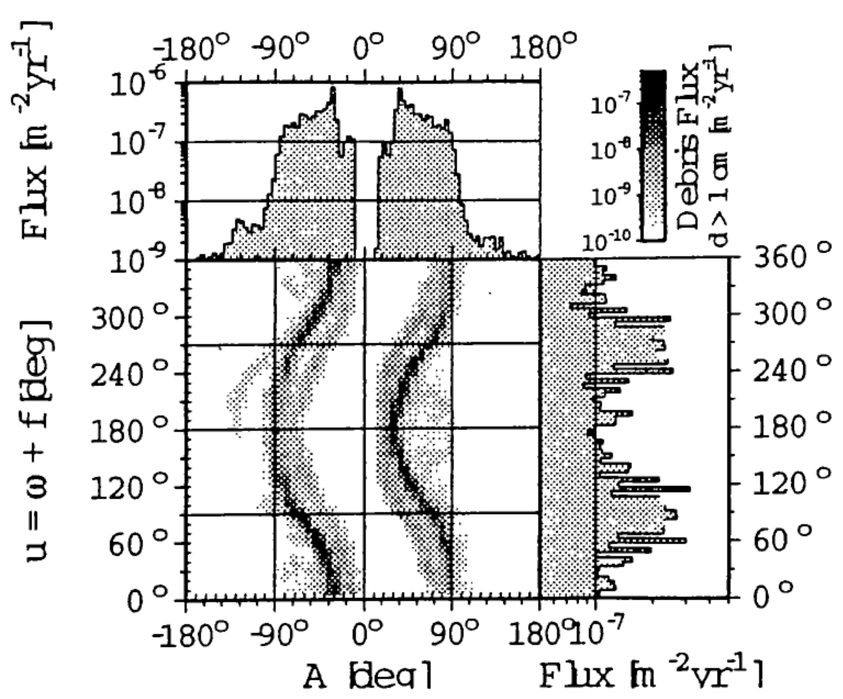

Fig.1: Jan.1997 LEO debris flux on ISS for $d > 1$ cm as function of impact azimuth A and orbit position $u = \omega + f$ (MASTER Analyst Model).

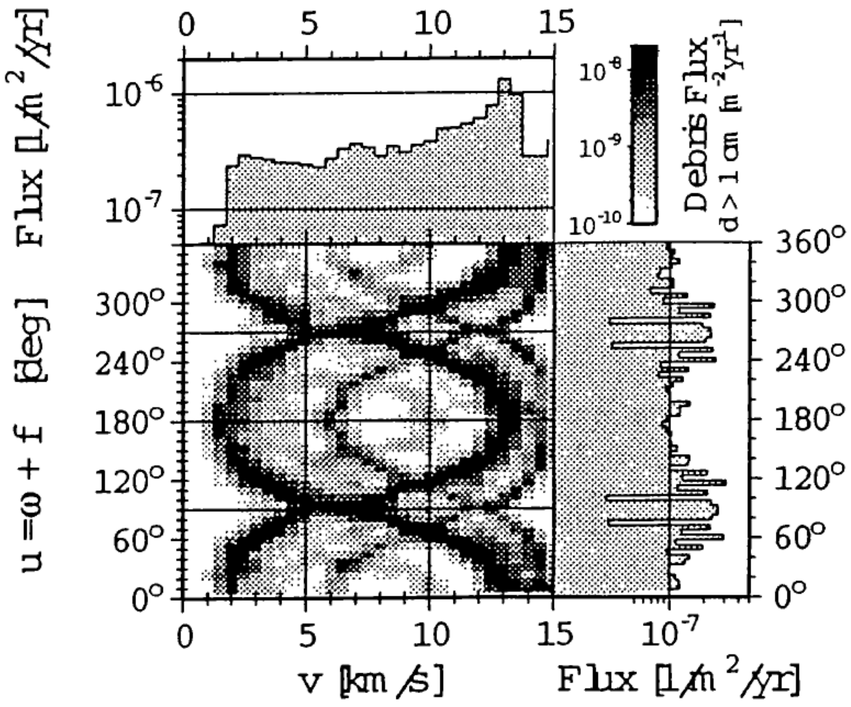

Fig.2: Jan.1997 LEO debris flux on ISS for $d > 1$ cm as function of impact velocity V and orbit position $u = \omega + f$ (MASTER Analyst Model).

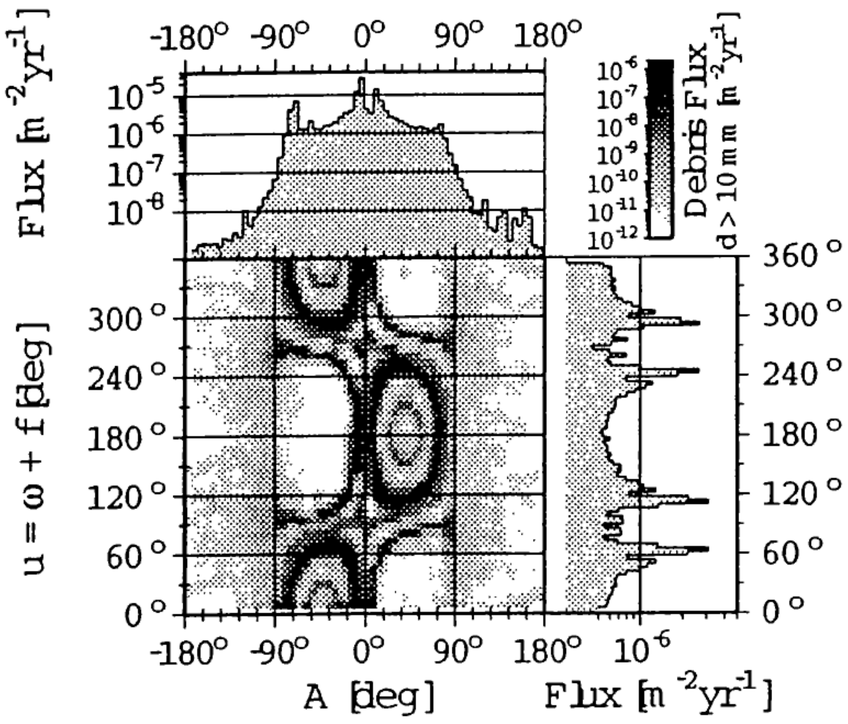

Fig.3: Jan.1997 LEO debris flux on ERS-1 for $d > 1$ cm as function of impact azimuth A and orbit position $u = \omega + f$ (MASTER Analyst Model).

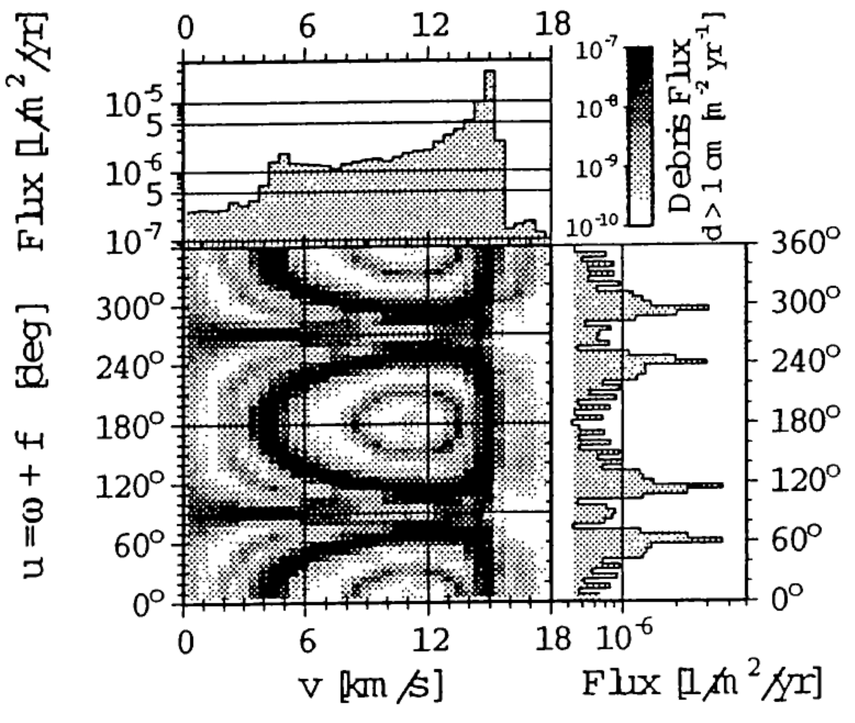

Fig.4: Jan.1997 LEO debris flux on ERS-1 for $d > 1$ cm as function of impact velocity V and orbit position $u = \omega + f$ (MASTER Analyst Model).

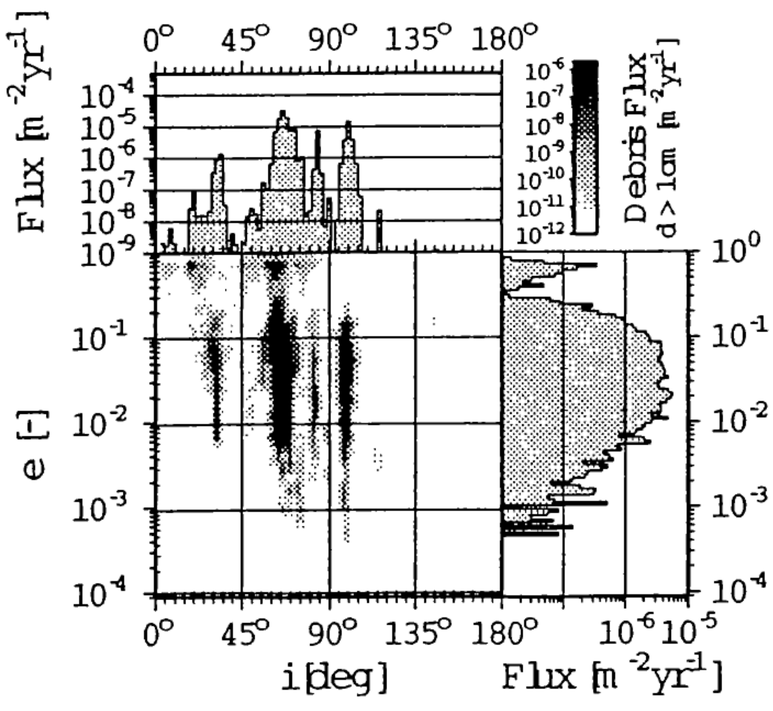

Fig.5: Jan.1997 LEO debris flux on ERS-1 for $d > 1$ cm as function of impactor orbit inclination i and eccentricity e (MASTER Analyst Model).

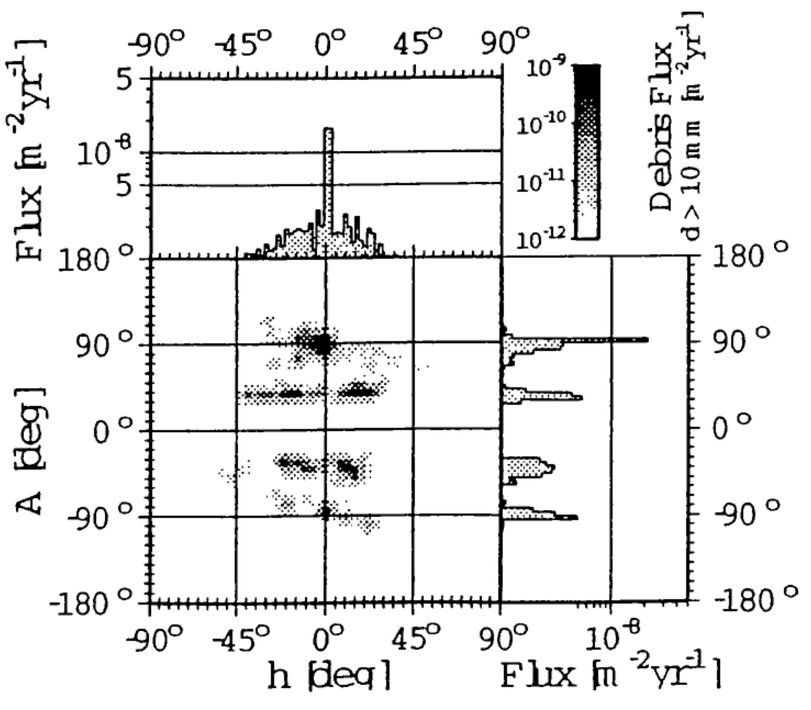

Fig.6: Jan.1997 GEO debris flux on Meteosat-5 for $d > 1$ cm as function of impact azimuth A and elevation h (MASTER Analyst Model).

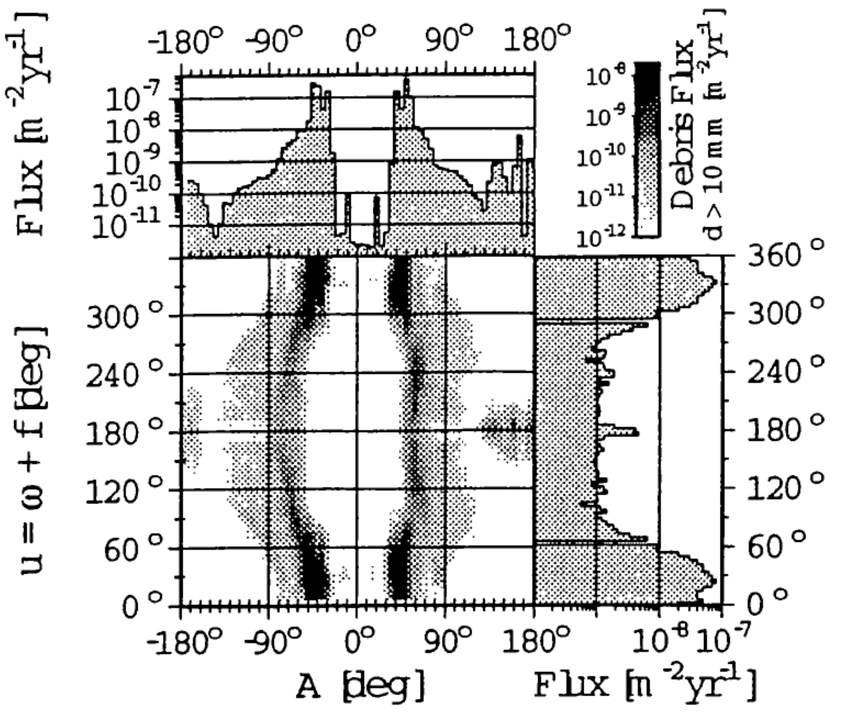

Fig.7: Jan.1997 GTO debris flux on Ariane-5 for $d > 1$ cm as function of impact azimuth A and orbit position $u = \omega + f$ (MASTER Analyst Model).

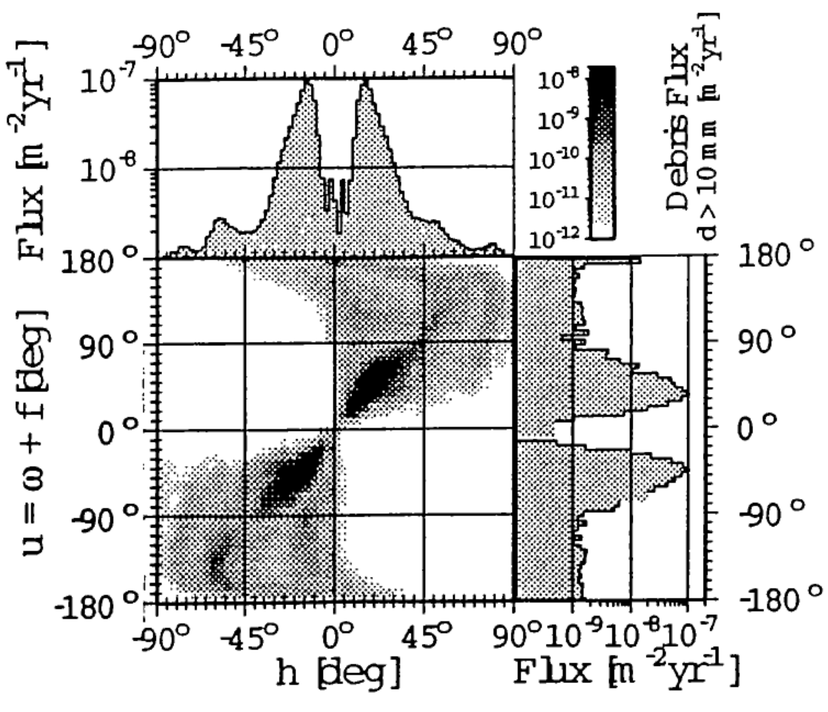

Fig.8: Jan.1997 GTO debris flux on Ariane-5 for $d > 1$ cm as function of impact elevation h and orbit position $u = \omega + f$ (MASTER Analyst Model).

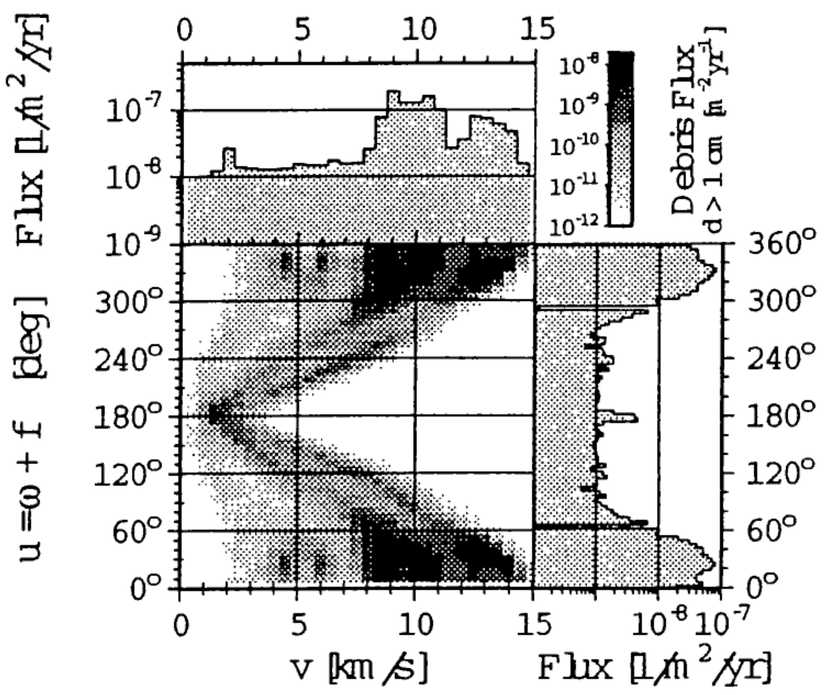

Fig.9: Jan.1997 GTO debris flux on Ariane-5 for $d > 1$ cm as function of impact velocity V and orbit position $u = \omega + f$ (MASTER Analyst Model).

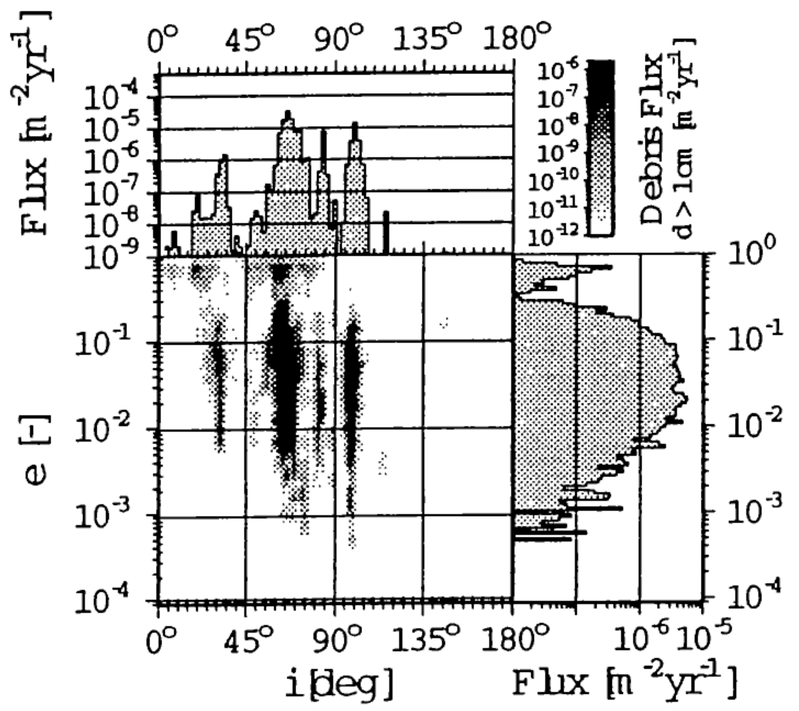

Fig.10: Jan.1997 GTO debris flux on Ariane-5 for $d > 1$ cm as function of impactor orbit inclination i and eccentricity e (MASTER Analyst Model).

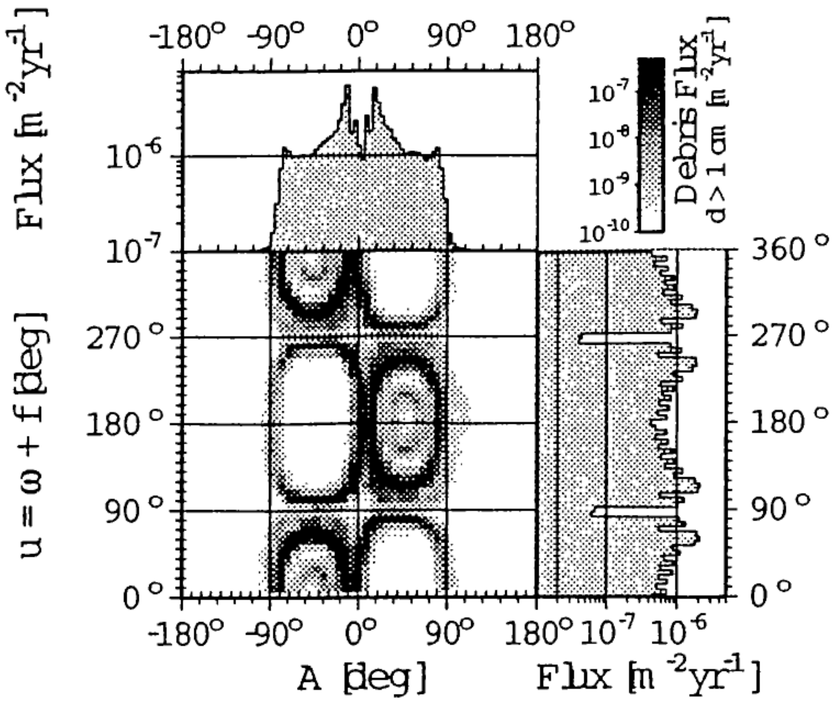

Fig.11: Jan.1997 LEO debris flux on Iridium for $d > 1$ cm as function of impact azimuth A and orbit position $u = \omega + f$ (MASTER Analyst Model).

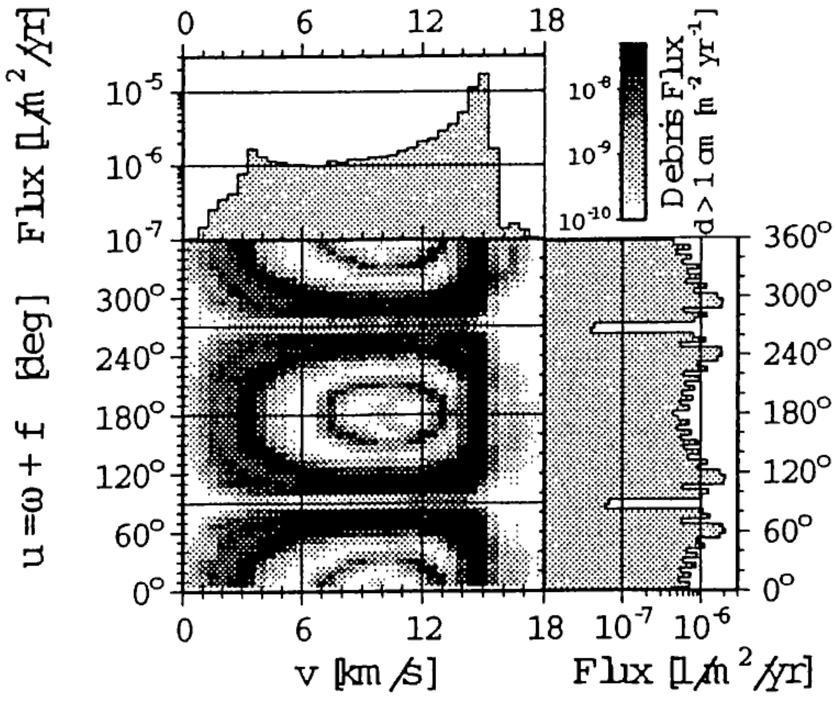

Fig.12: Jan.1997 LEO debris flux on Iridium for $d > 1$ cm as function of impact velocity V and orbit position $u = \omega + f$ (MASTER Analyst Model).

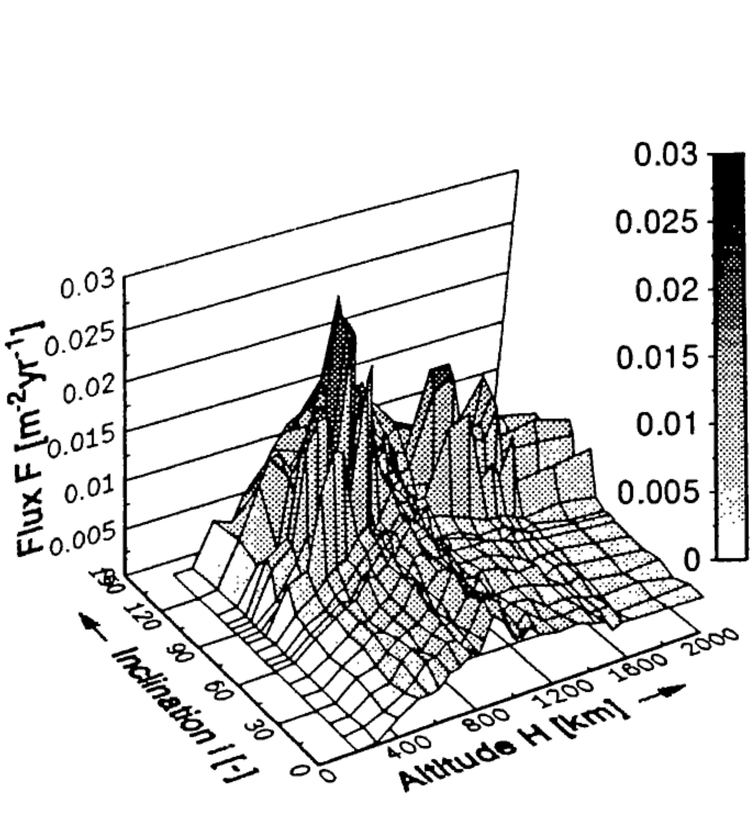

Fig.13: Jan.1997 LEO debris flux for $d > 1$ cm as function of the target orbit inclination i and mean altitude H (MASTER Engineering Model).

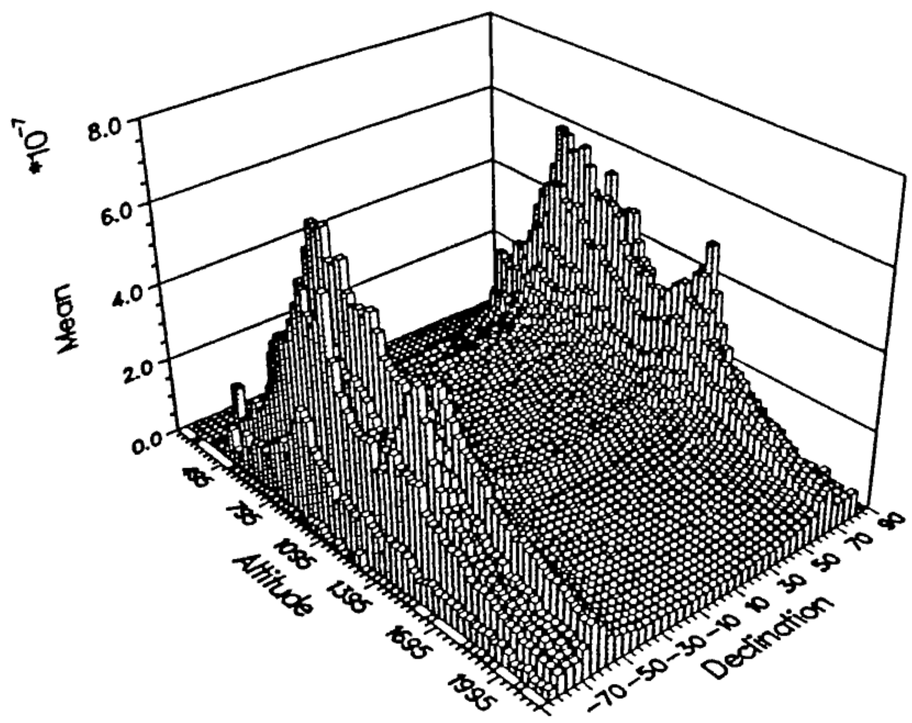

Fig.14 Jan.1997 spatial density distribution in LEO for $d > 1$ cm as function of mean altitude H and declination δ of (MASTER Analyst Model).

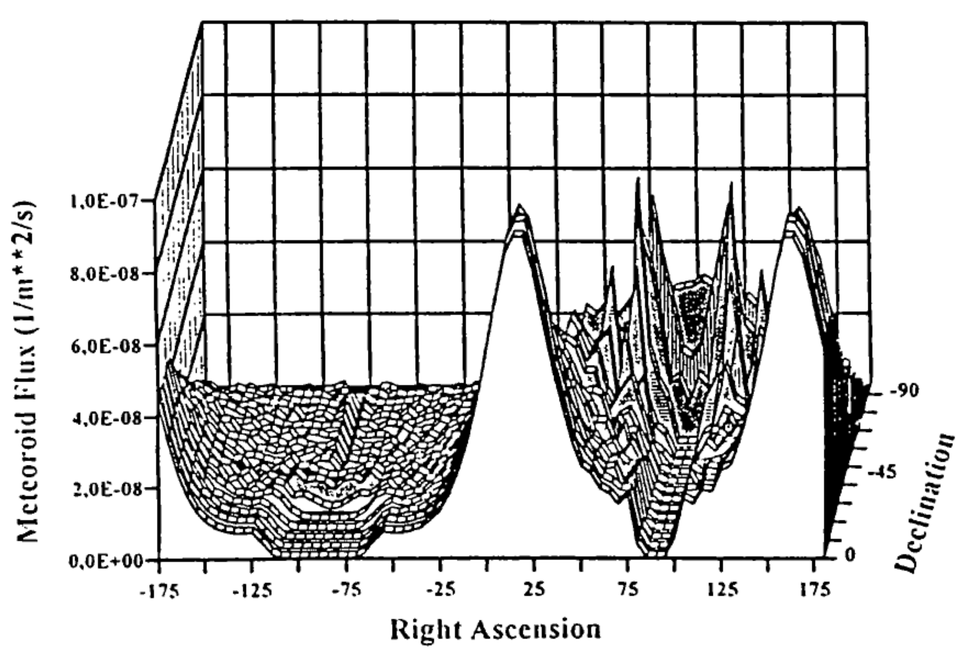

Fig.15: Meteoroid flux for $d > 0.1$ mm at a position trailing 20,000 km behind the earth on its orbit around the sun, as a function of impact direction (MASTER Analyst Model).

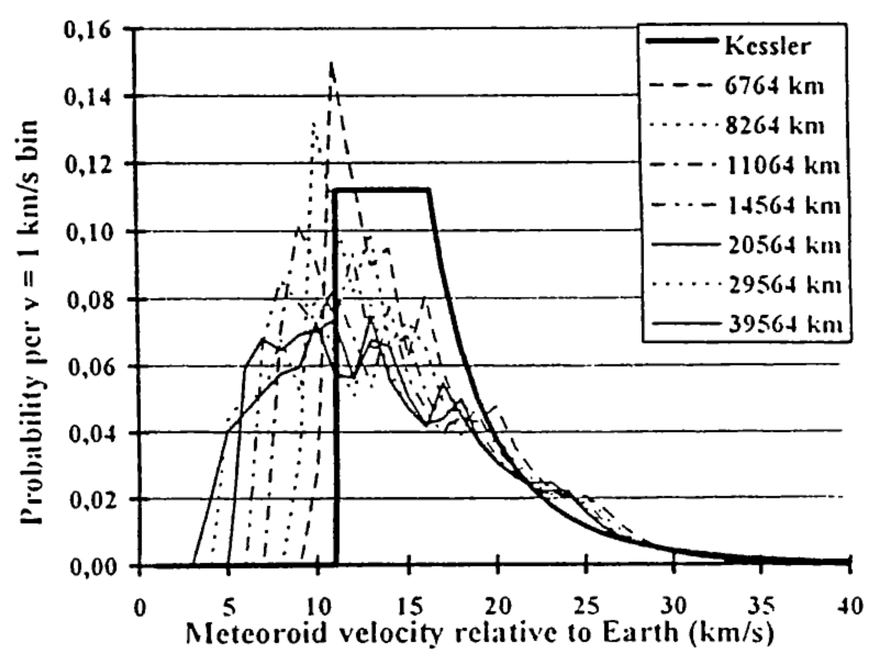

Fig.16: Probability distribution of meteoroid impact velocities as a function of the geocentric distance (gravitational focussing effect, MASTER Analyst Model).

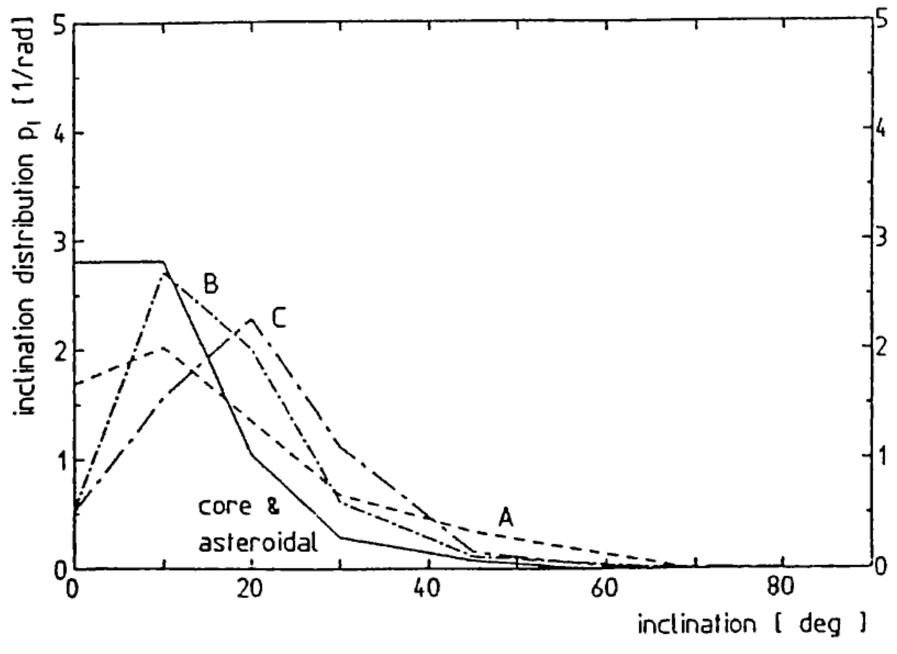

Fig.17: Probability distribution of meteoroid orbit inclinations for 5 different populations, described in a heliocentric ecliptic system (Staubach model).

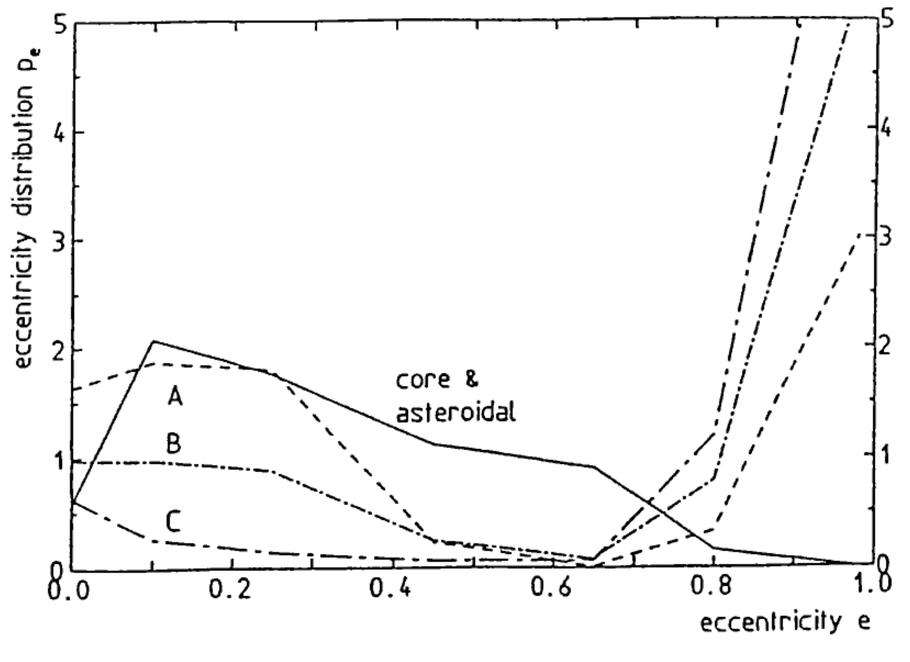

Fig.18: Probability distribution of meteoroid orbit eccentricities for 5 different populations, described in a heliocentric ecliptic system (Staubach model).